

# Signature of the time-dependent hydrodynamic interactions on the collective diffusion in colloidal monolayers

Alvaro Domínguez

*Física Teórica, Universidad de Sevilla, Apdo. 1065, 41080 Sevilla, Spain\**

(Dated: October 9, 2014)

It has been shown recently that the coefficient of collective diffusion in a colloidal monolayer is divergent due to the hydrodynamic interactions mediated by the ambient fluid in bulk. The analysis is extended to allow for time-dependent hydrodynamic interactions. Novel observational features specific to this time dependency are predicted. The possible experimental detection in the dynamics of the monolayer is discussed.

PACS numbers: 82.70.Dd, 47.57.eb, 05.70.Ln

## I. INTRODUCTION

A colloidal monolayer is formed when colloidal particles are constrained to stay in a surface. This confinement can be achieved in several manners: particles trapped by wetting forces at the interface between two fluids (typically, air and water, or oil and water) [1], non-buoyant particles sedimented at the bottom of a fluid phase [2], particles trapped by optical tweezers into predetermined configurations [3]. The monolayer behaves for most practical purposes as a two-dimensional (2D) system. This renders the monolayer a practical physical system to address fundamental questions experimentally that concern the role of the spatial dimensionality on the mechano-statistical properties of many-body systems. A nice illustration of this usefulness was the first experimental confirmation of the Kosterlitz-Thouless scenario for melting in 2D systems [2].

The dynamics of colloids may be strongly influenced by the hydrodynamic interactions mediated by the ambient fluid in which they are immersed (see, e.g., Ref. [4]). Therefore, although a colloidal monolayer is a 2D system, the dynamics may include a contribution from 3D hydrodynamic interactions by an unconfined ambient fluid. This configuration can be called “*partial confinement*” of the system “colloid + ambient fluid”, and it provides a different scenario from absence of confinement (i.e., 3D colloid in bulk) and from complete confinement (a monolayer embedded in a likewise confined fluid, e.g., in a slit pore or in a liquid film [5]).

Recently, the analysis of a theoretical model for the “partial confinement” configuration has shown [6] that, as a consequence of the hydrodynamic interactions, the collective diffusion in the monolayer is anomalous on spatial scales above a certain characteristic length  $L_{\text{hydro}}$ . This prediction has been confirmed experimentally by the measurement, through dynamic light scattering, of a diverging coefficient of collective diffusion [7, 8]. This unique feature of “partial confinement” (as opposed to absence of and to complete confinement) follows from the contribution of the long-ranged part of the hydrodynamic interactions in the linearized equation for density perturbations. This theoretical prediction assumes that the hydrodynamic interactions are established instantaneously. This is a good approximation in many experimental situations and simplifies considerably the theoretical modelling. However, there can be configurations in which the relaxation of the ambient flow vorticity cannot be neglected. In this work, the model introduced in Ref. [6] is extended to incorporate this effect. The analysis reveals a second characteristic length  $L_{\text{cross}}$  (much larger than  $L_{\text{hydro}}$ ), above which the dynamics of density perturbations crosses over to a non-diffusive behavior dominated by the time-dependency of the hydrodynamic interactions, that exhibits specific features associated to the “partial confinement”. This is actually a novel prediction for the observation of time-dependent hydrodynamic interactions, facilitated in this case by the configuration of “partial confinement”.

In Sec. II we introduce the extension of the theoretical model of Ref. [6] that incorporates the evolution of the velocity field in the ambient flow, modelled with the time-dependent Stokes equation. An equation for the evolution of the monolayer density is derived and solved in the limit of small deviations from homogeneity. Two opposite limiting cases of the solution are discussed, namely, the limit of instantaneous establishment of the hydrodynamic interaction (Sec. II A), so that the model of Ref. [6] is recovered, and the “thermodynamic limit” of density perturbations with infinite spatial extension (Sec. II B), so that the crossover length scale  $L_{\text{cross}}$  is probed by the dynamics. In Sec. III the possibility of the experimental observation of time-dependent hydrodynamic interactions via the monolayer dynamics is thoroughly discussed and estimates are provided for the relevant length and time scales in realistic experimental conditions. Sec. IV summarizes the conclusions.

---

\* dominguez@us.es

## II. THEORETICAL MODEL

We consider the simplest physical model that exhibits the relevant phenomenology as introduced in Ref. [6], namely a collection of particles restricted to move in the plane  $z = 0$  but subjected to the hydrodynamic interaction mediated by an ambient fluid filling the whole space. As discussed in Ref. [9], modifications of this model to describe more realistic experimental configurations (e.g., particles confined to the planar interface at  $z = 0$  between two different fluids) do not alter the qualitative picture. The following fields are defined (with  $\mathbf{r} = (x, y)$  denoting the position in the monolayer plane at  $z = 0$ ):

- (i) The 2D particle number density field,  $\varrho(\mathbf{r}, t)$ , in the monolayer plane.
- (ii) The in-plane (2D) velocity field,  $\mathbf{v}(\mathbf{r}, t)$ , of the flow of particles.
- (iii) The 3D velocity field,  $\mathbf{u}(\mathbf{r}, z, t)$ , of the flow of the ambient fluid.
- (iv) The average total force per particle,  $\mathbf{f}_{\text{tot}}(\mathbf{r}, t)$ , which is a “generalized” or “thermodynamic” force and accounts for the effect of Brownian diffusion, of the direct (“static”) interactions between the particles, and of the external and confining forces.

These fields are related to each other by the following equations, expressing physical laws and simplifying assumptions:

**(A)** Particle number conservation in the monolayer plane:

$$\frac{\partial \varrho}{\partial t} = -\nabla \cdot (\varrho \mathbf{v}), \quad \nabla := \left( \frac{\partial}{\partial x}, \frac{\partial}{\partial y} \right). \quad (1)$$

**(B)** Particle motion in the so-called *point-particle (Oseen) approximation*:

$$\mathbf{v}(\mathbf{r}, t) = \Gamma \mathbf{f}_{\text{tot}}(\mathbf{r}, t) + \mathbf{u}(\mathbf{r}, z = 0, t), \quad (2)$$

together with the time-dependent Stokes equation for incompressible flow (denoting  $\mathbf{x} := \mathbf{r} + z\mathbf{e}_z$  and  $\nabla_{\mathbf{x}} := \nabla + \mathbf{e}_z \partial_z$ ),

$$\rho_{\text{fluid}} \frac{\partial \mathbf{u}}{\partial t} = \eta \nabla_{\mathbf{x}}^2 \mathbf{u} - \nabla_{\mathbf{x}} p + \delta(z) \varrho(\mathbf{r}, t) \mathbf{f}_{\text{tot}}(\mathbf{r}, t), \quad (3a)$$

$$\nabla_{\mathbf{x}} \cdot \mathbf{u} = 0, \quad (3b)$$

with the boundary condition of vanishing fields at infinity. Here,  $\Gamma$  is the mobility of an isolated particle,  $\rho_{\text{fluid}}$  is the mass density of the ambient fluid,  $\eta$  its kinematic viscosity,  $p(\mathbf{x})$  is the pressure field enforcing the 3D incompressibility constraint (3b), and the Dirac delta in Eq. (3a) describes the geometrical confinement of the particles to the plane  $z = 0$ . Physically, Eq. (2) represents the motion of a particle in the overdamped regime under the effect of the total force as if isolated (Stokes drag) plus the advection by the ambient fluid flow, *evaluated at the confining plane*. The ambient flow, in turn, is determined by Eqs. (3) self-consistently in terms of the motion of the particles.

The point-particle approximation incorporates only the dominant contribution of the hydrodynamic interaction in the limit that the interparticle separation is much larger than the size and the hydrodynamic radius of the particles (dilute regime). It is possible to relax this hypothesis to some extent by allowing for a dependence of  $\Gamma$  on the density  $\varrho$ , which should account for the short-separation contributions by the hydrodynamic interaction (see, e.g., Refs. [10–15]). This would not affect, however, the conclusions [9].

This model for the ambient flow includes the diffusion of the vorticity in the regime of low Reynolds and Mach numbers. This is the point of departure from the model addressed in Refs. [6, 9], which assumes that the ambient flow adapts instantaneously to a given particle configuration (i.e., one sets  $\partial_t \mathbf{u} = 0$  in Eq. (3a)).

**(C)** Particles are confined to the plane  $z = 0$ , i.e.,  $\mathbf{e}_z \cdot \mathbf{v}(\mathbf{r}, t) = 0$ , implying from Eq. (2) that

$$\mathbf{e}_z \cdot \mathbf{f}_{\text{tot}}(\mathbf{r}, t) = -\frac{1}{\Gamma} \mathbf{e}_z \cdot \mathbf{u}(\mathbf{r}, z = 0, t). \quad (4)$$

It is straightforward to show that if the pair  $\{\mathbf{u}(\mathbf{r}, z, t), \mathbf{f}_{\text{tot}}(\mathbf{r}, t)\}$  satisfies Eqs. (3), so does the specular reflection with respect to the plane  $z = 0$  (i.e., the pair obtained by the transformation  $z \rightarrow -z$ ,  $u_z \rightarrow -u_z$ ,  $\mathbf{e}_z \cdot \mathbf{f}_{\text{tot}} \rightarrow -\mathbf{e}_z \cdot \mathbf{f}_{\text{tot}}$ , everything else unchanged). Therefore, a solution to Eq. (4) is

$$\mathbf{e}_z \cdot \mathbf{f}_{\text{tot}}(\mathbf{r}, t) = 0 \quad (5)$$

by continuity of the velocity field  $\mathbf{u}$  at  $z = 0$ . Physically, if the net force on the particles points in the confining plane, their motion only induces, in the point-particle approximation, an in-plane ambient flow when evaluated at the plane.

The condition expressed by Eq. (5) is actually an equation for the unknown constraining force, that can be used to eliminate any explicit mention to this force in the model equations: one can replace  $\mathbf{f}_{\text{tot}}(\mathbf{r}, t)$  in Eqs. (2,3) by the projection onto the  $z = 0$  plane of all the forces other than the constraining force (i.e., Brownian, interparticle, and external). We denote this projection simply as  $\mathbf{f}(\mathbf{r}, t)$ , which by construction points in the confining plane.

(D) This latter force  $\mathbf{f}(\mathbf{r}, t)$  is assumed to be given as a function solely of the density field  $\varrho(\mathbf{r}, t)$ . A usual implementation of this assumption is the approximation of local thermal equilibrium, i.e., at each point the colloidal monolayer is assumed locally in intrinsic local equilibrium, and the flow of particles is driven by gradients of the local chemical potential as given by thermodynamics (and thus given as a function of the local density at the isothermal conditions appropriate for a colloid):

$$\mathbf{f} = -\nabla\mu = -\left(\frac{\partial\mu}{\partial\varrho}\right)_T \nabla\varrho. \quad (6)$$

More sophisticated approximations to the functional form of  $\mathbf{f}$  can be used in order to get expressions valid in a wider range of length scales or in situations very far from equilibrium. However, here only Eq. (6) will be used for simplicity, because it suffices to illustrate the phenomenology we are interested in.

In conclusion, Eqs. (1–6) form a closed set of equations for the evolution of the monolayer as described by the density field  $\varrho(\mathbf{r}, t)$ . Assuming that there are no external force fields,  $\mathbf{f}(\mathbf{r})$  will vanish in a homogeneous state,  $\varrho(\mathbf{r}, t) = \varrho_{\text{hom}}$ , so that the latter is a stationary solution of the model equations. They can be linearized about this reference solution,  $\varrho(\mathbf{r}, t) = \varrho_{\text{hom}} + \delta\varrho(\mathbf{r}, t)$  with  $|\delta\varrho| \rightarrow 0$ , so that

$$\frac{\partial\delta\varrho}{\partial t} \approx -\Gamma\varrho_{\text{hom}}\nabla\cdot\delta\mathbf{f} - \varrho_{\text{hom}}\nabla\cdot\mathbf{u}(\mathbf{r}, z=0), \quad (7a)$$

$$\rho_{\text{fluid}}\frac{\partial\mathbf{u}}{\partial t} \approx \eta\nabla_{\mathbf{x}}^2\mathbf{u} - \nabla_{\mathbf{x}}p + \delta(z)\varrho_{\text{hom}}\delta\mathbf{f}(\mathbf{r}, t), \quad (7b)$$

$$\nabla_{\mathbf{x}}\cdot\mathbf{u} = 0, \quad (7c)$$

$$\delta\mathbf{f} \approx -\frac{D_0}{\Gamma\varrho_{\text{hom}}}\nabla\delta\varrho, \quad (7d)$$

$$D_0 := \Gamma\varrho_{\text{hom}}\left(\frac{\partial\mu}{\partial\varrho}\right)_T (\varrho = \varrho_{\text{hom}}). \quad (7e)$$

The coefficient of collective diffusion,  $D_0$ , can be related to the isothermal compressibility of the monolayer in the reference homogeneous state (see Eq. (D1)). Although one usually considers  $D_0 > 0$  (the reference homogeneous state is stable), it is also of interest to consider the influence of the hydrodynamic interactions on the dynamics of an unstable state,  $D_0 < 0$  (an example of experimental relevance is the clustering in a monolayer under the effect of capillary attraction [6, 16–19]). Therefore, in the calculations in the rest of the paper no assumption will be made concerning the sign of  $D_0$ .

It is instructive to discuss how Eqs. (7) would be modified in the cases of absence of or complete confinement, respectively. The key issue is that, although the 3D ambient flow is incompressible, see Eq. (7c), the continuity equation for the monolayer incorporates only the ambient flow *in the monolayer plane*,  $z = 0$ , see Eq. (7a), and this needs not be incompressible. This fact and the long-ranged nature of the hydrodynamic interactions co-act to yield a divergent correction of the coefficient of collective diffusion in the limit of instantaneous hydrodynamic interactions [6]. In the absence of confinement (i.e., 3D continuity equation in 3D ambient flow) or in the case of complete confinement (2D continuity equation in 2D ambient flow), there would be no explicit dependence on the ambient velocity field  $\mathbf{u}$  in the linearized continuity equation due to the incompressibility constraint. This does not mean that hydrodynamic interactions would not affect diffusion, but only that this would occur through nonlinear corrections or, more generally, through mode-coupling terms that would also incorporate the short-range contributions by the hydrodynamic interactions. Explicit calculations and simulations of a 3D colloid (see, e.g., Refs. [10–15]) show that these effects lead at most to a finite renormalization of the diffusion coefficient in the form of a density-dependent mobility, as mentioned briefly before.

In order to solve Eqs. (7), one introduces the Laplace transform in time and the Fourier transform in the spatial variables:

$$\hat{\varrho}(\mathbf{k}, s) := \int_0^{+\infty} dt e^{-st} \int d^2\mathbf{r} e^{-i\mathbf{k}\cdot\mathbf{r}} \delta\varrho(\mathbf{r}, t), \quad (8a)$$

$$\hat{\mathbf{u}}(\mathbf{k}, q, s) := \int_0^{+\infty} dt e^{-st} \int d^2\mathbf{r} \int_{-\infty}^{+\infty} dz e^{-i\mathbf{k}\cdot\mathbf{r}-iqz} \mathbf{u}(\mathbf{r}, z, t). \quad (8b)$$

For an initial condition  $\varrho(\mathbf{r}, t=0) = \varrho_0(\mathbf{r})$ ,  $\mathbf{u}(\mathbf{r}, z, t=0) = \mathbf{0}$ , Eqs. (7) become

$$s\hat{\varrho}(\mathbf{k}, s) - \hat{\varrho}_0(\mathbf{k}) \approx -D_0 k^2 \hat{\varrho}(\mathbf{k}, s) - \varrho_{\text{hom}} \int_{-\infty}^{+\infty} \frac{dq}{2\pi} i\mathbf{k} \cdot \hat{\mathbf{u}}(\mathbf{k}, q, s), \quad (9a)$$

$$[\rho_{\text{fluid}} s + \eta(k^2 + q^2)] \hat{\mathbf{u}}(\mathbf{k}, q, s) \approx -\frac{D_0}{\Gamma} \left[ \mathcal{I} - \frac{(\mathbf{k} + q\mathbf{e}_z)(\mathbf{k} + q\mathbf{e}_z)}{k^2 + q^2} \right] \cdot (i\mathbf{k}) \hat{\varrho}(\mathbf{k}, s). \quad (9b)$$

One can evaluate the integral term in Eq. (9a):

$$\begin{aligned} \int_{-\infty}^{+\infty} \frac{dq}{2\pi} i\mathbf{k} \cdot \hat{\mathbf{u}}(\mathbf{k}, q, s) &= \frac{D_0 k^2}{\Gamma} \hat{\varrho}(\mathbf{k}, s) \int_{-\infty}^{+\infty} \frac{dq}{2\pi} \frac{q^2}{[k^2 + q^2] [\rho_{\text{fluid}} s + \eta(k^2 + q^2)]} \\ &= \frac{D_0 k^2 \hat{\varrho}(\mathbf{k}, s)}{\varrho_{\text{hom}}} \mathcal{H}(k, s), \end{aligned} \quad (10)$$

where we have defined the auxiliary function

$$\mathcal{H}(k, s) := \frac{2}{L_{\text{hydro}} k} \left[ 1 + \sqrt{1 + \frac{\tau_{\omega} s}{(L_{\text{hydro}} k)^2}} \right]^{-1}, \quad (11)$$

in terms of the length scale

$$L_{\text{hydro}} := \frac{4\eta\Gamma}{\varrho_{\text{hom}}}, \quad (12)$$

introduced in Ref. [6], and the time scale

$$\tau_{\omega} := \frac{\rho_{\text{fluid}} L_{\text{hydro}}^2}{\eta}, \quad (13)$$

associated to the relaxation of the ambient vorticity on the length scale  $L_{\text{hydro}}$ . The solution of Eq. (9a) is written as

$$\hat{\varrho}(\mathbf{k}, s) = \hat{\varrho}_0(\mathbf{k}) \hat{G}(k, s), \quad (14)$$

with the Green function

$$\hat{G}(k, s) := \frac{1}{s + D_0 k^2 [1 + \mathcal{H}(k, s)]}. \quad (15)$$

Thus, the function  $\mathcal{H}(k, s)$  encodes the effect of the hydrodynamic interactions on the dynamics of the monolayer.

The goal is to study the analytical properties of the Green function  $\hat{G}(k, s)$  and, more interestingly, of its inverse Laplace transform, given by the Mellin formula,

$$G(k, t > 0) = \int_{\mathcal{C}} \frac{ds}{2\pi i} e^{st} \hat{G}(k, s), \quad (16a)$$

with the integration path

$$\mathcal{C} := \{ \text{Re } s = p > 0 \text{ constant and to the right of any singularity in the complex } s\text{-plane} \}. \quad (16b)$$

As we shall see,  $G(k, t)$  is directly related to the experimentally relevant intermediate scattering function. Its dependence on  $t$  is controlled by the structure in the complex  $s$ -plane of the function  $\hat{G}(k, s)$ . This is analyzed in App. A and here we summarize the relevant conclusions. A crossover length scale, associated to the time scale  $\tau_{\omega}$ , appears naturally as

$$L_{\text{cross}} := \frac{L_{\text{hydro}}^3}{\tau_{\omega} |D_0|}. \quad (17)$$

Notice that, unlike  $L_{\text{hydro}}$ , this length scale depends on the specific form of the interaction potential between the particles through the value of the diffusion coefficient  $D_0$ . It can be assumed that  $L_{\text{hydro}} < L_{\text{cross}}$  (actually,  $L_{\text{hydro}} \ll L_{\text{cross}}$  in realistic configurations, see the discussion in Sec. III). In the complex  $s$ -plane (see left part of Fig. 3), the function  $\hat{G}(k, s)$  has a branch cut discontinuity in the negative real axis with a branching point at

$$s_{\text{branch}} = -\frac{(L_{\text{hydro}}k)^2}{\tau_\omega}, \quad (18)$$

and either (i) a single real pole if  $D_0 < 0$ , or if  $D_0 > 0$  and  $L_{\text{cross}}k \gtrsim 1$ , or (ii) two complex conjugate poles if  $D_0 > 0$  and  $L_{\text{cross}}k \lesssim 1$ . Consequently, the inversion in Eq. (16) is written as the sum of a contribution by the poles and a contribution by an integral along the branch discontinuity, see Eq. (A6). Although this general expression can be applied to study the two cases, it is physically more illuminating to consider two limiting situations which provide the correct qualitative picture, namely, the limit  $L_{\text{cross}} \rightarrow \infty$  for case (i), interpreted as  $\tau_\omega \rightarrow 0$  or time-independent hydrodynamic interactions, and the limit  $k \rightarrow 0$  for case (ii), interpreted as the “thermodynamic limit”.

### A. Time-independent hydrodynamic interactions

In the limiting case in which the hydrodynamic interactions are established instantaneously, one recovers the results presented in Ref. [6]. This limit means that the time  $\tau_\omega$  is much shorter than any other time of interest and corresponds mathematically to the limit  $\tau_\omega \rightarrow 0$  in the Green function: from Eq. (11), one gets  $\mathcal{H}(k, s) \sim \mathcal{H}(k, 0) = 1/(L_{\text{hydro}}k)$  and from Eq. (15),

$$\hat{G}(k, s) \sim \frac{1}{s + D_0k^2[1 + \mathcal{H}(k, 0)]}. \quad (19)$$

It is useful to introduce the  $k$ -dependent time scales

$$\tau_0(k) := \frac{1}{|D_0|k^2} \quad (20)$$

(corresponding to normal diffusion) and

$$\tau_1(k) := \frac{\tau_0}{\mathcal{H}(k, 0)} = \frac{L_{\text{hydro}}}{|D_0|k}. \quad (21)$$

Therefore, since the Green function in Eq. (19) has only a simple pole in  $s$ , Eq. (16) predicts an exponential dependence in time,

$$G(k, t) = e^{-(\text{sign } D_0)t \left[ \frac{1}{\tau_0} + \frac{1}{\tau_1} \right]}. \quad (22)$$

(That is, the inversion of the Laplace transform is dominated by the contribution of the single pole in the real axis; the contribution of the branch cut discontinuity is negligible because the branching point moves to infinity in the limit  $\tau_\omega \rightarrow 0$ , see Eq. (18)). The meaning of the length scale  $L_{\text{hydro}}$  defined in Eq. (12) is now clear: if  $L_{\text{hydro}}k \gg 1$ , the evolution of the Fourier modes is controlled by the time scale  $\tau_0(k)$  and they follow normal diffusion with a constant  $D_0$  (actually, “antidiffusion” if  $D_0 < 0$ ). In the opposite case,  $L_{\text{hydro}}k \ll 1$  and the evolution is controlled by the time scale  $\tau_1(k)$ , so that the Fourier modes exhibit anomalous diffusion (superdiffusion, to be more precise), i.e., exponential dependence in time with a diffusion coefficient diverging as  $k \rightarrow 0$ . Physically, the length scale  $L_{\text{hydro}}$  separates the regimes when the evolution of the monolayer density is dominated, in Eq. (7a) or in Eq. (9a), by diffusion properly (and one approximates  $1 + \mathcal{H}(k, 0) \approx 1$  in Eq. (19)) or by advection by the time-independent ambient flow (and  $1 + \mathcal{H}(k, 0) \approx \mathcal{H}(k, 0)$  in Eq. (19)).

It is clear from Eq. (11) that the approximation  $\tau_\omega \rightarrow 0$  and the “thermodynamic” limit,  $k \rightarrow 0$ , do not commute. Since the inverse Laplace transform is controlled by the pole at  $s = -\text{sign } D_0/\tau_1(k)$  when setting  $\tau_\omega = 0$ , the previous conclusions are valid provided  $k$  is small but still large enough that it holds

$$\left. \frac{\tau_\omega |s|}{(L_{\text{hydro}}k)^2} \right|_{s=1/\tau_1(k)} \ll 1 \quad \Leftrightarrow \quad 1 \ll L_{\text{cross}}k, \quad (23)$$

in terms of the crossover length scale defined by Eq. (17). Therefore, the regime of anomalous diffusion described by Eq. (22) must be interpreted as an intermediate asymptotics,  $L_{\text{hydro}} \ll k^{-1} \ll L_{\text{cross}}$ . Physically, the restriction in Eq. (23) means that the ambient vorticity of mode  $k$  relaxes much faster than the characteristic time scale of particle diffusion over a length scale  $\sim k^{-1}$ . If this scale is so large that  $L_{\text{cross}}k \ll 1$ , however, one cannot neglect the dynamical evolution of the ambient fluid vorticity. This is addressed next.

## B. Time-dependent hydrodynamic interactions

Consider now the “thermodynamic limit”, i.e., the limit  $k \rightarrow 0$  of the Green function without the restriction described by Eq. (23). As shown in App. B, both the branch point and the singularities of  $\hat{G}(k, s)$  approach zero as  $k \rightarrow 0$ , whereby a new time scale appears naturally that is defined as

$$\tau_2(k) := \left( \frac{\tau_\omega}{4|D_0|^2 k^4} \right)^{1/3}, \quad (24)$$

to be compared with  $\tau_0(k)$  and  $\tau_1(k)$  in Eqs. (20, 21). The inversion in Eq. (16) is thus dominated by the behavior of the Green function near  $s = 0$  in the limit  $k \rightarrow 0$ , so that one can approximate  $1 + \mathcal{H}(k, s) \sim 1 + \mathcal{H}(0, s) \sim \mathcal{H}(0, s) = 2/\sqrt{\tau_\omega s}$  and

$$\hat{G}(k, s) \sim \frac{1}{s + D_0 k^2 \mathcal{H}(0, s)}. \quad (25)$$

Physically, this means that the evolution of the monolayer density is dominated, in Eq. (7a) or in Eq. (9a), by advection by the ambient flow, in turn determined by neglecting the in-plane shear in Eq. (7b) or in Eq. (9b), but not the time dependence.

The evaluation of the Mellin formula (16) with the approximation (25) is described in App. B. The result is summarized in the scaling behavior

$$G(k, t) = \gamma \left( \frac{t}{\tau_2(k)} \right), \quad (26a)$$

with the scaling function

$$\gamma(u) = \begin{cases} \frac{4}{3} e^{-u/2} \cos \frac{\sqrt{3}}{2} u - I(u), & D_0 > 0, \\ \frac{2}{3} e^u + I(u), & D_0 < 0, \end{cases} \quad (26b)$$

where [20]

$$I(u) := \frac{1}{\pi} \int_0^\infty dx \frac{\sqrt{x}}{x^3 + 1} e^{-ux}. \quad (26c)$$

Unlike in the limiting case addressed in the previous subsection, the contribution of the branch cut is now as important as the one by the singularities of the Green function.

Figures 1 and 2 show plots of the scaling function  $\gamma(u)$ . Some relevant properties are derived in App. C: the function  $\gamma(u)$  is regular and infinitely differentiable if  $u > 0$ ; at  $u = 0$ , its second derivative does not exist, behaving as

$$\gamma(u \rightarrow 0) \sim 1 - \frac{4 \text{sign } D_0}{3\sqrt{\pi}} u^{3/2}. \quad (27)$$

In the opposite limit one has the asymptotic behavior

$$\gamma(u \rightarrow +\infty) \sim \begin{cases} -\frac{1}{2\sqrt{\pi} u^{3/2}}, & D_0 > 0, \\ \frac{2}{3} e^u, & D_0 < 0. \end{cases} \quad (28)$$

When  $D_0 > 0$ , the oscillatory behavior in time of  $G(k, t)$  (with a characteristic time  $\tau_2(k)$ ) and the long-time algebraic decay,  $G(k, t) \sim t^{-3/2}$ , are the signatures of the time dependence of the hydrodynamic interactions. If  $D_0 < 0$ ,  $G(k, t)$  grows exponentially in time, as in the absence of hydrodynamic interactions, but the time dependence of the hydrodynamic interaction shows up in the specific  $k$ -dependence of the characteristic time scale,  $\tau_2 \propto k^{-4/3}$ .

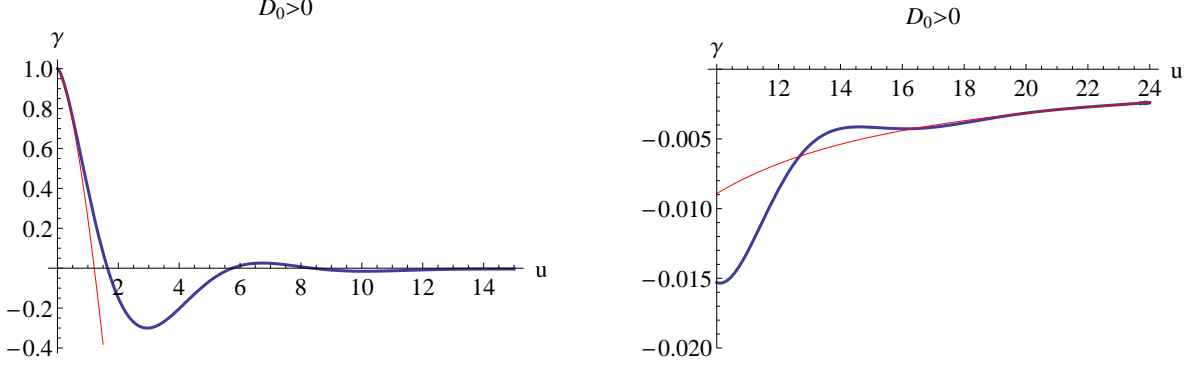


FIG. 1. The scaling function  $\gamma(u)$  for  $D_0 > 0$  given by Eq. (26b) (thick, blue line), together with the predicted asymptotic behaviors for small and large values of the argument, see Eqs. (27) and (28) respectively (thin, red lines).

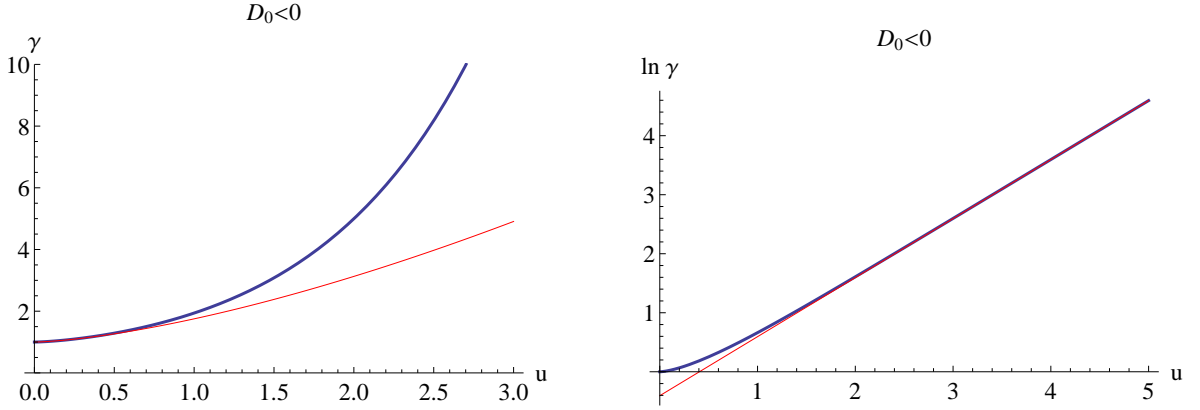


FIG. 2. Same as Fig. 1 but for  $D_0 < 0$ .

### III. FEASIBILITY OF EXPERIMENTAL OBSERVATION

The Green function  $G(k, t)$  has an immediate relationship with experimentally accessible quantities because it is basically the intermediate scattering function  $F(k, t)$  of the monolayer, which can be measured with dynamic light scattering experiments [4]. If the monolayer consists of  $N$  particles, the function  $F(k, t)$  is defined in terms of an ensemble average over equilibrium configurations as [21]

$$F(k, t) := \frac{1}{N} \langle \hat{\rho}(\mathbf{k}, t) \hat{\rho}(-\mathbf{k}, 0) \rangle = G(k, t) S(k), \quad (29)$$

when Eq. (14) is applied. Here, the structure factor  $S(k) := \langle |\hat{\rho}_0(\mathbf{k})|^2 \rangle / N$  is independent of the hydrodynamic interactions and determined completely by thermodynamic equilibrium. If  $k^{-1}$  is larger than the equilibrium correlation length, one can approximate  $S(k)$  by a constant and the relevant dependence on  $k$  and  $t$  is determined completely by the Green function.

The results of the previous Section can be summarized in the following three expected regimes for the intermediate scattering function (for definiteness, we assume the case of a stable reference state, i.e.,  $D_0 > 0$ ):

- (1) *Regime of negligible hydrodynamic interactions*,  $k^{-1} \ll L_{\text{hydro}}$ : the function  $F(k, t)$  exhibits normal diffusive behavior, i.e., exponential decay in time with a characteristic time that scales as  $k^{-2}$ , see Eq. (20), so that it is possible to define a diffusion coefficient.
- (2) *Regime of dominant instantaneous hydrodynamic interactions*,  $L_{\text{hydro}} \ll k^{-1} \ll L_{\text{cross}}$ : the function  $F(k, t)$  still decays exponentially in time, but with a characteristic time that scales as  $k^{-1}$ , see Eq. (21), and satisfying

$$\frac{\tau_1(k)}{\tau_\omega} = \frac{L_{\text{cross}}}{L_{\text{hydro}}} \frac{1}{L_{\text{hydro}} k} \gg 1. \quad (30a)$$

Therefore, it is possible to define a  $k$ -dependent diffusion coefficient, but not a diffusion constant as the limit  $k \rightarrow 0$ .

- (3) *Regime of dominant time-dependent hydrodynamic interactions*,  $L_{\text{cross}} \ll k^{-1}$ : the function  $F(k, t)$  exhibits

damped oscillations and algebraic decay in time (see Fig. 1) with a characteristic time that scales as  $k^{-4/3}$ , see Eq. (24), and satisfying

$$\frac{\tau_2(k)}{\tau_\omega} = \left( \frac{L_{\text{cross}}}{L_{\text{hydro}}} \right)^2 \frac{1}{(\sqrt{2}L_{\text{cross}}k)^{4/3}} \gg 1. \quad (30b)$$

Therefore, the dynamics of the monolayer density cannot be characterized as diffusive at all.

In order to provide quantitative estimates, we consider by way of example a collection of spherical colloidal particles (radius  $R$ ) immersed in water at room temperature, for which  $\eta \approx 10^{-3}$  N s/m<sup>2</sup>,  $\rho_{\text{fluid}} \approx 10^3$  kg/m<sup>3</sup>. The 2D packing fraction of the colloid is denoted as  $\phi = \pi R^2 \varrho_{\text{hom}}$ . The particle mobility  $\Gamma$  can depend on  $\phi$  in order to account for the effect of the short-distance hydrodynamic interactions; this would amount to replacing  $\Gamma$  by  $\Gamma(\varrho = \varrho_{\text{hom}})$  in Eqs. (7). To our knowledge, however, there are no studies of this dependency in the case of monolayers. For bulk colloids, plenty of works have shown that the specific interparticle forces will affect this dependency, also whether  $\Gamma$  decreases or increases with  $\phi$  (see, e.g., Refs. [12, 14, 15, 22]). Therefore, it is difficult to advance a conjecture on the behavior of the function  $\Gamma(\phi)$  for a monolayer. Here, we simply assume (without convincing justification, however) that the variation of  $\Gamma$  with  $\phi$  is less than an order of magnitude, as is the case in bulk colloids. Thus, one can take the value of  $\Gamma$  for an isolated particle (dilute limit) for reference purposes: this can be estimated with Stoke's drag formula for no-slip boundary conditions as  $\Gamma \approx 1/(6\pi\eta R)$ . Finally, the diffusion coefficient  $D_0$  will also depend on  $\phi$  according to the interparticle forces; this dependency is studied in App. D for several realistic models. For reference purposes, we quote its value for an ideal gas at room temperature,  $D_{\text{ideal}} \approx 0.04\Gamma \times 10^{-19}$  J, see Eq. (D2). However, unlike  $\Gamma$ , the coefficient  $D_0$  can change with  $\phi$  by orders of magnitude (see Fig. 6).

With these choices for the parameter values, the relevant length scales of the model are estimated as

$$\frac{L_{\text{hydro}}}{\mu\text{m}} \approx \frac{2}{3\phi} \frac{R}{\mu\text{m}}, \quad (31a)$$

$$\frac{L_{\text{cross}}}{\mu\text{m}} \approx \frac{3 \times 10^6}{\phi} \frac{D_{\text{ideal}}}{D_0(\phi)} \left( \frac{R}{\mu\text{m}} \right)^2, \quad (31b)$$

and the relevant time scales are

$$\frac{\tau_\omega}{\text{s}} \approx \frac{0.4 \times 10^{-6}}{\phi^2} \left( \frac{R}{\mu\text{m}} \right)^2, \quad (31c)$$

$$\frac{\tau_2(k = 1/L_{\text{cross}})}{\text{s}} \approx \frac{6 \times 10^6}{\phi^2} \left( \frac{D_{\text{ideal}}}{D_0(\phi)} \right)^2 \left( \frac{R}{\mu\text{m}} \right)^4. \quad (31d)$$

Several observations are in order:

(i) The ratio

$$\frac{L_{\text{cross}}}{L_{\text{hydro}}} \approx \frac{5 \times 10^6}{\phi} \frac{D_{\text{ideal}}}{D_0(\phi)} \frac{R}{\mu\text{m}}, \quad (32)$$

will be very large in any case, also for the smallest colloidal particles,  $R \sim 1$  nm. Therefore, the separation of scales,  $L_{\text{hydro}} \ll L_{\text{cross}}$ , assumed in the theoretical analysis holds under realistic conditions.

(ii) The length scale  $L_{\text{hydro}}$  is much larger than the mean interparticle separation,  $\ell \sim R/\sqrt{\phi}$ , only for a dilute system. A dense system has  $L_{\text{hydro}} \sim \ell$ , and therefore the regime of normal collective diffusion,  $k^{-1} \ll L_{\text{hydro}}$ , would be masked in such case presumably by single-particle effects.

(iii) The time scale for relaxation of the velocity of a single particle, on which the overdamped approximation (2) is based, can be estimated as  $\tau_{\text{relax}} \sim \varrho_{\text{fluid}} R^2 / \eta$  (see, e.g., [4]), so that  $\tau_\omega / \tau_{\text{relax}} \sim (L_{\text{hydro}}/R)^2 \sim \phi^{-2}$ . Therefore,  $\tau_\omega > \tau_{\text{relax}}$  and, in view of Eqs. (30), the relevant time scales are consistent with the approximation of overdamped motion.

The anomalous diffusion predicted in the intermediate regime  $L_{\text{hydro}} \ll k^{-1} \ll L_{\text{cross}}$  has been observed experimentally: the reinterpretation of old experimental data obtained through dynamic light scattering [7] allows one to conclude that the coefficient of collective diffusion diverges [8]. The monolayer of this experiment can be modelled as a collection of hard disks of radius  $R \approx 120$  nm, the probed values of the packing fraction being in the range  $\phi \approx 0.12 - 0.57$ . The above estimates give the range  $L_{\text{hydro}} \approx 0.1 - 0.7 \mu\text{m}$ ,  $L_{\text{cross}} \approx 6 - 200 \text{ nm}$ ,  $\tau_2(k = 1/L_{\text{cross}}) \approx 10 - 10^5 \text{ s}$  for



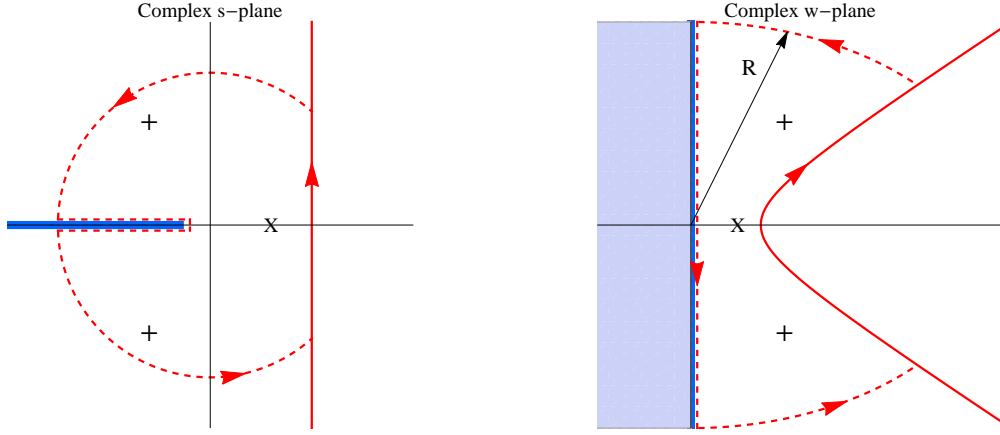


FIG. 3. Analytical structure of  $\hat{G}(k, s)$ . The complex  $s$ -plane (left) and the complex  $w$ -plane (right) are related by the conformal transformation (A1). The thick blue line in the  $s$ -plane is the branch cut, which is transformed into the excluded region  $\text{Re } w < 0$  in the  $w$ -plane. The symbols indicate the relative positions of the singularities of  $\hat{G}(k, s)$ : “+” when  $D_0 > 0$  and  $k < k_c$ , “X” when  $D_0 < 0$  or when  $D_0 > 0$  and  $k_c < k$ . The red line is the integration path in the Mellin formula (Eq. (16) or Eq. (A3)); the dashed red lines correspond to the paths  $K_R$  and  $L_R$  (see Eq. (A6)) completing the original path into a closed contour.

this experimental configuration, so that the crossover to the regime of time-dependent hydrodynamic interactions is technically unobservable. However, it is possible to reduce the values of  $L_{\text{cross}}$  and  $\tau_2$  by considering smaller particles or a denser monolayer. For instance, a monolayer formed by charged nanoparticles with  $R \sim 10$  nm, at high densities ( $\phi \sim 1$ ) such that one could assume  $D_0/D_{\text{ideal}} \sim 10^2$  (see Fig. 6), is predicted to have  $L_{\text{hydro}} \sim 7$  nm,  $L_{\text{cross}} \sim 3$   $\mu\text{m}$  and  $\tau_2(k = 1/L_{\text{cross}}) \sim 6$   $\mu\text{s}$ . Therefore, the observation of the crossover and of the signature by the time-dependent hydrodynamic interactions on the intermediate scattering function, see Fig. 1, should be within reach of up-to-date experimental techniques. Actually, given that  $L_{\text{cross}}$  can have values in the micrometer range, the effect of ambient vortex relaxation on the collective dynamics could be relevant, beyond light scattering observations, for the macroscopic rheological properties of the monolayer.

#### IV. CONCLUSIONS

We have generalized the result on anomalous diffusion in colloidal monolayers derived in Ref. [6] by including the relaxational dynamics of the vorticity in the ambient fluid. In this expanded framework, the result predicted in Ref. [6] and observed experimentally in Ref. [7, 8] must be understood as an intermediate asymptotic behavior. Two well separated length scales,  $L_{\text{hydro}}$  and  $L_{\text{cross}}$ , have been identified that separate three dynamical regimes in the evolution of the monolayer: on spatial scales well below  $L_{\text{hydro}}$ , the effect of the hydrodynamic interactions mediated by the ambient fluid is negligible. On scales between  $L_{\text{hydro}}$  and  $L_{\text{cross}}$ , the collective dynamics of the monolayer is dominated by the hydrodynamic interactions as if instantaneous, and the model of Ref. [6] is recovered. Finally, on scales well above  $L_{\text{cross}}$  a novel dynamical regime is predicted where the time dependency of the hydrodynamic interactions is relevant. We have discussed how each regime would appear in the experimentally accessible intermediate scattering function. We have provided a detailed discussion of the influence of the system parameters on the values of the lengths  $L_{\text{hydro}}$  and  $L_{\text{cross}}$ , and of the possible observation of the features specific to the different dynamical regimes.

#### Appendix A: Analytic structure of $\hat{G}(k, s)$

The presence of a square root in the definition of the function  $\hat{G}(k, s)$ , see Eqs. (11, 15), implies that it is defined in the complex  $s$ -plane with a branching point, see Eq. (18), and cut along the negative real axis between the branching point and  $-\infty$ , see Fig. 3. It is useful to define a conformal transformation to a new complex variable as

$$w = \sqrt{1 - \frac{s}{s_{\text{branch}}}}, \quad (\text{A1})$$

that maps the cut  $s$ -plane into the half-plane  $\text{Re } w > 0$ . We introduce the auxiliary quantities

$$\sigma := \text{sign } D_0, \quad (\text{A2a})$$

$$\lambda := \sigma \frac{L_{\text{hydro}}}{L_{\text{cross}}} = \frac{\tau_\omega D_0}{L_{\text{hydro}}^2}, \quad (\text{A2b})$$

$$k_c := \frac{2\sigma}{L_{\text{cross}}}(1 - \lambda)^{-1}, \quad (\text{A2c})$$

in terms of the length scales defined in Eqs. (12, 17), so that the Mellin formula (16) becomes

$$G(k, t > 0) = \int_{\mathcal{C}'} dw \xi(w, t), \quad (\text{A3a})$$

with the integrand

$$\xi(w, t) := \frac{w(1+w)e^{(1-w^2)ts_{\text{branch}}}}{i\pi P(w)}, \quad (\text{A3b})$$

$$P(w) := w^3 + w^2 - (1 - \lambda)w + (1 - \lambda) \left( \frac{k_c}{k} - 1 \right), \quad (\text{A3c})$$

and the transformed integration path

$$\mathcal{C}' := \{ \text{Re } (w^2 - 1) = p' > 0 \}, \quad (\text{A3d})$$

i.e., the branch of the hyperbole  $(\text{Re } w)^2 - (\text{Im } w)^2 = 1 + p'$  in the half-plane  $\text{Re } w > 0$  and to the right of any singularity of the integrand, see Fig. 3. These singularities are given by the roots of the polynomial  $P(w)$  with non-negative real part (possibly barring the non-generic cases that  $w = 0$  or  $w = -1$  are roots). In order to analyze the character of the roots, we assume  $L_{\text{hydro}} < L_{\text{cross}}$ , so that  $-1 < \lambda < +1$  and  $1 - \lambda > 0$  (actually, as argued in Sec. III, the physically relevant situations correspond to  $|\lambda| \ll 1$ ). Several cases can be distinguished:

**(1)** Either  $\sigma = -1$ , or  $\sigma = +1$  and  $k > k_c$ : although  $k_c$  can have any sign, it is  $(1 - \lambda)(k_c/k - 1) < 0$ . Therefore, application of Descartes' rule of signs to the polynomial  $P(w)$  allows one to conclude that there is always a positive real root. The other two roots are either negative or complex conjugate of each other. In any case, the sum of the three roots must equal  $-1$  (minus the coefficient of  $w^2$  in  $P(w)$ ), so that their real parts must be negative and they are thus irrelevant. In conclusion, the only relevant singularity in the  $w$ -plane is a simple pole on the positive real axis.

**(2)**  $\sigma = +1$  and  $k < k_c$ : now  $k_c > 0$  and  $(1 - \lambda)(k_c/k - 1) > 0$ , and Descartes' rule of signs leads to the conclusion that there is one negative, and thus irrelevant root. The other two roots are either positive or complex conjugate of each other. To clarify this issue, consider the positions of the local extrema of  $P(w)$ , given as

$$P'(w) = 0 \Rightarrow w_{\pm} = \frac{1}{3} \left[ -1 \pm \sqrt{1 + 3(1 - \lambda)} \right], \quad (\text{A4})$$

with  $w_- < 0$  and  $w_+ > 0$ . Qualitatively,  $P(w)$  has the graph shown in Fig. 4, so that two positive roots can only exist provided  $P(w_+) < 0$ . One defines  $k_+$  by the condition  $P(w_+) = 0$ ; although an explicit expression for  $k_+$  as a function of  $\lambda$  can be written down, it suffices with the plot in Fig. 5, showing that, for all practical purposes, one can assume  $k_+ \approx k_c$ . Therefore, ignoring the narrow range  $k_+ < k < k_c$  where the polynomial  $P(w)$  has two positive roots, the roots will be complex conjugate of each other. One can further show that, in such case, their real part is positive: denoting the roots as  $w_1, w_2, w_3$ , with  $w_1 < 0$ ,  $w_3^* = w_2$ , one can inspect the coefficient of  $w$  in  $P(w)$ :

$$w_1 w_2 + w_1 w_3 + w_2 w_3 = 2w_1 \text{Re } w_2 + |w_2|^2 = -(1 - \lambda) < 0, \quad (\text{A5})$$

so that  $\text{Re } w_2 > 0$  necessarily. In conclusion, the relevant singularities are two complex conjugate simple poles in the half-plane  $\text{Re } w > 0$ .

The pole structure of  $\hat{G}(k, s)$  is summarized Fig. 3. The Mellin formula in Eq. (A3) can be written in terms of explicit real Riemann integrals by application of the theorem of the residues: one builds a closed contour as indicated

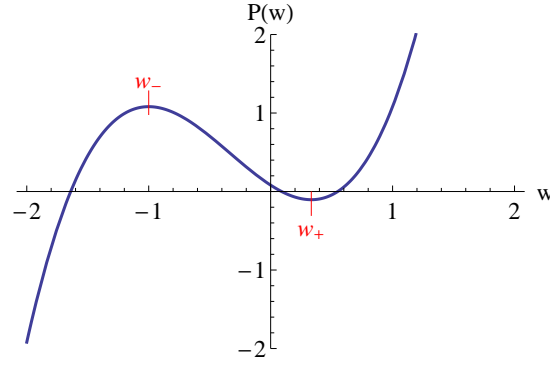


FIG. 4. Graph of the polynomial  $P(w)$  defined by Eq. (A3c) for generic values of the parameters  $\lambda > 0$  and  $k$ . Note that changes in  $k$  amount just to a vertical shift of the graph. The positions of the local extrema,  $w_{\pm}$ , are given by Eq. (A4).

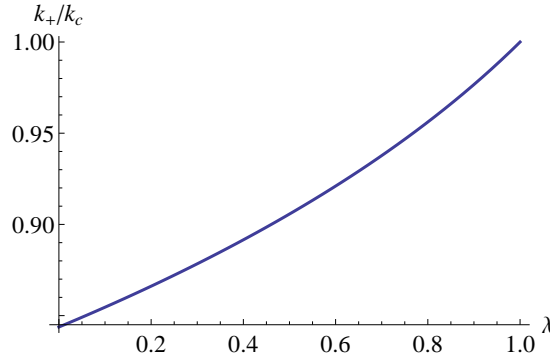


FIG. 5. Plot of  $k_+/k_c$  as function of  $\lambda > 0$ , where  $k_+$  is given by the condition  $P(w_+) = 0$ .

in Fig. 3 in the limit  $R \rightarrow \infty$ , consisting of a straight line along the (transformed) branch cut ( $L_R$  at  $\text{Re } w = 0^+$ ) and two arcs of circle (of radius  $R$  and denoted  $K_R$ ) joining the straight line with the hyperbole  $\mathcal{C}'$ . Then, Eq. (A3) can be written as

$$G(k, t) = 2\pi i \sum_n \text{Res}_{w_n} \xi(w, t) - \lim_{R \rightarrow \infty} \int_{K_R \cup L_R} dw \xi(w, t). \quad (\text{A6})$$

The residues contribute either a real exponential when  $D_0 < 0$  or when  $D_0 > 0$  and  $k_c < k$  (case 1 above), or exponentially damped oscillations when  $D_0 > 0$  and  $k_c < k$  (case 2). The integral along the arcs  $K_R$  vanishes in the limit  $R \rightarrow \infty$ , as follows from a standard application of Jordan's lemma (which is more easily done in terms of the original variable  $s$  in the Mellin formula in Eq. (16)). The integral along the straight line,  $L_R := \{w = iy \mid |y| < R\}$  in the sense of decreasing  $y$ , can be simplified after some algebraic manipulations and a change to the new integration variable  $x = y^2$ :

$$\lim_{R \rightarrow \infty} \int_{L_R} dw \xi(w, t) = \frac{1 - \lambda k_c}{\pi k} \int_0^\infty dx \frac{\sqrt{x} e^{(1+x)t s_{\text{branch}}}}{|P(i\sqrt{x})|^2}, \quad (\text{A7a})$$

where

$$\begin{aligned} |P(i\sqrt{x})|^2 &= x^3 + (3 - 2\lambda)x^2 + (1 - \lambda) \left( 3 - \lambda - \frac{2k_c}{k} \right) x \\ &\quad + (1 - \lambda)^2 \left( \frac{k_c}{k} - 1 \right)^2. \end{aligned} \quad (\text{A7b})$$

### Appendix B: Green function in the limit $k \rightarrow 0$

Here Eqs. (26) are derived. In the limit  $k \rightarrow 0$ , the roots of  $P(w)$  are given by the approximate equation (see Eq. (A3c))

$$P(w) \approx w^3 + (1 - \lambda) \frac{k_c}{k} = 0. \quad (\text{B1})$$

Since  $1 - \lambda > 0$ , the solutions of this equation in the half-plane  $\text{Re } w > 0$  depend on the sign of  $D_0$  (through the sign of  $k_c$ , see Eqs. (A2)):

$$w = \left[ (1 - \lambda) \frac{|k_c|}{k} \right]^{1/3} \times \begin{cases} 1 & \text{if } D_0 < 0, \\ e^{\pm i\pi/3} & \text{if } D_0 > 0. \end{cases} \quad (\text{B2})$$

Therefore, from Eqs. (18, A1) one deduces the position of the singularities of  $\hat{G}(k, s)$  in the complex  $s$ -plane as  $k \rightarrow 0$ :

$$s = \frac{1}{\tau_2(k)} \times \begin{cases} 1 & \text{if } D_0 < 0, \\ e^{\pm i2\pi/3} & \text{if } D_0 > 0, \end{cases} \quad (\text{B3})$$

in terms of the time scale  $\tau_2(k)$  defined by Eq. (24).

The inversion of the approximated Green function (25) with the Mellin formula (16) is facilitated by performing the change of variable  $z = \sqrt{s\tau_2(k)}$ . This is nothing else but the conformal transformation (A1) in the limit  $k \rightarrow 0$  with an appropriate rescaling so that the singularities have a finite position in this limit, see Eq. (B3). With this new variable, Eqs. (16, 25) lead to Eq. (26a) where

$$\gamma(u) := \frac{1}{i\pi} \int_{\hat{\mathcal{C}}} dz \frac{z^2}{z^3 + \sigma} e^{uz^2}, \quad (\text{B4a})$$

with the transformed integration path

$$\hat{\mathcal{C}} := \{\text{Re } z^2 = \hat{p} > 0\}, \quad (\text{B4b})$$

i.e., the branch of the hyperbole  $(\text{Re } z)^2 - (\text{Im } z)^2 = \hat{p}$  in the half-plane  $\text{Re } z > 0$  and to the right of any singularity.

The expression of  $\gamma(u)$  in Eq. (26b) follows from the evaluation of the integral (B4) by closing the contour  $\hat{\mathcal{C}}$  as in Eq. (A6) (see Fig. 3). This gives a contribution of the poles and a contribution  $I(u)$ , see Eq. (26c), of the integral along the (transformed) branch cut  $\text{Re } z = 0^+$ . Of course, these expressions could have been obtained alternatively by taking the limit  $k \rightarrow 0$  in the exact expressions (A6, A7).

### Appendix C: Properties of the function $\gamma(u)$

The function  $\gamma(u)$  defined by Eq. (B4) can be expressed as in Eq. (26b). Since the integrals

$$\frac{d^n I}{du^n} = \frac{1}{\pi} \int_0^\infty dx \frac{(-x)^n \sqrt{x}}{x^3 + 1} e^{-ux} \quad (\text{C1})$$

converge for any  $n$  if  $u > 0$ , the function  $\gamma(u)$  and its derivatives exist for any  $u > 0$ . To obtain the behavior as  $u \rightarrow 0$ , one writes the function  $I(u)$  as follows:

$$\begin{aligned} I(u) &= \frac{1}{\pi} \int_0^\infty dx \frac{\sqrt{x}}{1+x^3} (1-ux) + \frac{1}{\pi} \int_0^\infty dx \frac{\sqrt{x}}{1+x^3} (e^{-ux} - 1 + ux) \\ &= \frac{1-2u}{3} + \frac{u^{3/2}}{\pi} \int_0^\infty d\xi \frac{\sqrt{\xi}}{u^3 + \xi^3} (e^{-\xi} - 1 + \xi) \\ &\stackrel{u \rightarrow 0}{\sim} \frac{1-2u}{3} + \frac{u^{3/2}}{\pi} \int_0^\infty d\xi \frac{\sqrt{\xi}}{\xi^3} (e^{-\xi} - 1 + \xi) \\ &\sim \frac{1}{3} \left( 1 - 2u + \frac{4}{\sqrt{\pi}} u^{3/2} \right). \end{aligned} \quad (\text{C2})$$

Inserting this result in Eq. (26b) and expanding further in  $u \rightarrow 0$ , one arrives at Eq. (27). Actually, one can show that  $\gamma(u)$  has an expansion in powers of  $u^{3/2}$  about  $u = 0$ : changing the integration variable to  $\zeta = z\sqrt{u}$  in the definition (B4), one has

$$\gamma(u) = \frac{1}{i\pi} \int_{\mathfrak{C}} d\zeta \frac{\zeta^2 e^{-\zeta^2}}{\zeta^3 + \sigma u^{3/2}}, \quad \mathfrak{C} = \{\text{Re } \zeta^2 = 1\}, \quad (\text{C3})$$

where the integration path  $\mathfrak{C}$  can be taken to be  $u$ -independent because the singularities of the new integrand approach zero as  $u \rightarrow 0$ . Since  $|\zeta| \neq 0$  along the integration path, one can Taylor-expand the integrand uniformly as  $u \rightarrow 0$  and obtain

$$\gamma(u) = \frac{1}{i\pi} \int_{\mathfrak{C}} d\zeta \frac{e^{-\zeta^2}}{\zeta} \sum_{n=0}^{\infty} \left( -\sigma \frac{u^{3/2}}{\zeta^3} \right)^n = \sum_{n=0}^{\infty} a_n u^{3n/2},$$

$$a_n := \frac{(-\sigma)^n}{i\pi} \int_{\mathfrak{C}} d\zeta \frac{e^{-\zeta^2}}{\zeta^{1+3n}}. \quad (\text{C4a})$$

In the opposite limit,  $u \rightarrow +\infty$ , one notices that the function  $I(u)$  is formally analogous to a Laplace transform, see Eq. (26c), whose asymptotic behavior can be evaluated with Laplace's method [23]:

$$I(u) \sim \frac{1}{\pi} \int_0^{\infty} dx \sqrt{x} e^{-ux} = \frac{u^{-3/2}}{2\sqrt{\pi}}. \quad (\text{C5})$$

Therefore, this algebraic decay dominates over the exponential decay when  $\text{sign } D_0 = +1$ , but is subdominant compared to the exponential growth when  $\text{sign } D_0 = -1$ . In this manner, Eq. (28) is obtained.

#### Appendix D: The coefficient $D_0$ in different fluid models

By using thermodynamic identities, Eq. (7e) can be written as

$$D_0 = \Gamma \left( \frac{\partial p}{\partial \varrho} \right)_T (\varrho = \varrho_{\text{hom}}), \quad (\text{D1})$$

in terms of the equation of state  $p(\varrho, T)$  for the 2D pressure of the colloidal monolayer. In the dilute limit, the ideal gas approximation provides

$$D_0 = D_{\text{ideal}} = \Gamma T \quad (\text{D2})$$

(with the temperature  $T$  given in units of energy).

If the monolayer can be modelled as a collection of hard disks of radius  $R$ , its equation of state can be approximated by the expression [24]

$$p = \varrho T \frac{\varrho_c + \varrho}{\varrho_c - \varrho}, \quad (\text{D3})$$

with  $\varrho_c = (2\sqrt{3}R^2)^{-1}$  the number density for close packing of disks. From here one gets the ratio

$$\frac{D_0}{D_{\text{ideal}}} = \frac{2}{(1 - \phi/\phi_{\text{max}})^2} - 1. \quad (\text{D4})$$

in terms of the maximum packing fraction,  $\phi_{\text{max}} \approx 0.91$ , assuming a  $\phi$ -independent value of the mobility  $\Gamma$  (see the discussion in Sec. III). This function is plotted in Fig. 6.

Another realistic model of the monolayer is as a collection of particles with a soft repulsion, described by the potential

$$V(r) = T \left( \frac{\zeta}{r} \right)^3. \quad (\text{D5})$$

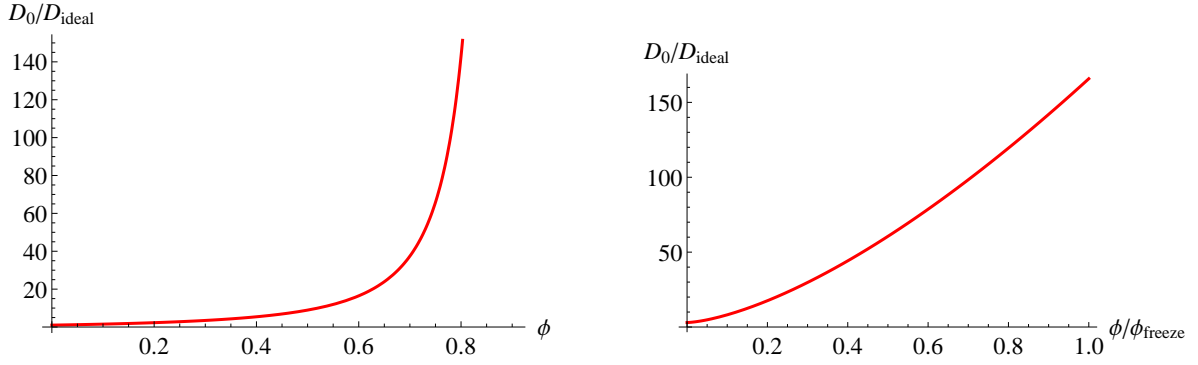


FIG. 6. (Left) The ratio  $D_0/D_{\text{ideal}}$  for a 2D fluid of hard disks, see Eq. (D4), as a function of the packing fraction  $\phi$  (which is  $\approx 0.91$  at close packing). (Right) The ratio  $D_0/D_{\text{ideal}}$  for a 2D fluid with Eq. (D5) as interparticle potential, as a function of  $\phi/\phi_{\text{freeze}}$ , where  $\phi_{\text{freeze}} \approx 14.45(R/\zeta)^2$  is the packing fraction at the freezing transition.

Here,  $\zeta$  is the associated Bjerrum length, which must be substantially larger than  $R$  so that the interparticle repulsion is indeed dominated by Eq. (D5) rather than by hard-core effects. This potential describes the large-separation dominant part of the electrostatic repulsion between charged particles located at the interface between a dielectric fluid and an electrolytic solution [25–28] and between polarizable particles in an external electric field [29, 30], and also the repulsion between superparamagnetic particles in an external magnetic field [31]. The equation of state associated to this potential can be computed using Montecarlo simulations [16] and the results for the ratio  $D_0/D_{\text{ideal}}$  are plotted in Fig. 6 (assuming again a  $\phi$ -independent mobility).

- 
- [1] B. P. Binks, *Curr. Opinion Coll. Interface Sci.* **7**, 21 (2002).
  - [2] K. Zahn, R. Lenke, and G. Maret, *Phys. Rev. Lett.* **82**, 2721 (1999).
  - [3] C. Lutz, M. Kollmann, and C. Bechinger, *Phys. Rev. Lett.* **93**, 026001 (2004).
  - [4] J. K. G. Dhont, *An Introduction to Dynamics of Colloids* (Elsevier Science, 1996).
  - [5] R. Di Leonardo, S. Keen, F. Ianni, J. Leach, M. J. Padgett, and G. Ruocco, *Phys. Rev. E* **78**, 031406 (2008).
  - [6] J. Bleibel, A. Domínguez, F. Günther, J. Harting, and M. Oettel, *Soft Matter* **10**, 2945 (2014).
  - [7] B. Lin, S. A. Rice, and D. A. Weitz, *Phys. Rev. E* **51**, 423 (1995).
  - [8] B. Lin, B. Cui, X. Xu, R. Zangi, H. Diamant, and S. A. Rice, *Phys. Rev. E* **89**, 022303 (2014).
  - [9] J. Bleibel, A. Domínguez, and M. Oettel, *J. Phys.: Condensed Matt.* (accepted) (2014).
  - [10] G. Batchelor, *J. Fluid Mech.* **52**, 245 (1972).
  - [11] J. F. Brady and L. J. Durlofsky, *Phys. Fluids* **31**, 717 (1988).
  - [12] M. Tokuyama and I. Oppenheim, *Phys. Rev. E* **50**, R16 (1994).
  - [13] M. Tokuyama and I. Oppenheim, *Physica A* **216**, 85 (1995).
  - [14] H. Hayakawa and K. Ichiki, *Phys. Rev. E* **51**, R3815 (1995).
  - [15] A. Moncho-Jordá, A. A. Louis, and J. T. Padding, *Phys. Rev. Lett.* **104**, 068301 (2010).
  - [16] A. Domínguez, M. Oettel, and S. Dietrich, *Phys. Rev. E* **82**, 011402 (2010).
  - [17] J. Bleibel, S. Dietrich, A. Domínguez, and M. Oettel, *Phys. Rev. Lett.* **107**, 128302 (2011).
  - [18] J. Bleibel, A. Domínguez, M. Oettel, and S. Dietrich, *Eur. Phys. J. E* **34**, 125 (2011).
  - [19] J. Bleibel, A. Domínguez, M. Oettel, and S. Dietrich, *Soft Matter* **10**, 4091 (2014).
  - [20] This function can actually be written in terms of a generalized hypergeometric function.
  - [21] J.-P. Hansen and I. R. McDonald, *Theory of Simple Liquids* (Academic Press, 1986).
  - [22] R. Piazza, *Rep. Prog. Phys.* **77**, 056602 (2014).
  - [23] C. M. Bender and S. A. Orszag, *Advanced Mathematical Methods for Scientists and Engineers* (McGraw-Hill, 1978).
  - [24] E. L. Grossman, T. Zhou, and E. Ben-Naim, *Phys. Rev. E* **55**, 4200 (1997).
  - [25] A. J. Hurd, *J. Phys. A: Math. Gen.* **18**, L1055 (1985).
  - [26] R. Aveyard, J. H. Clint, D. Nees, and V. N. Paunov, *Langmuir* **16**, 1969 (2000).
  - [27] A. Domínguez, D. Frydel, and M. Oettel, *Phys. Rev. E* **77**, 020401(R) (2008).
  - [28] K. D. Danov and P. A. Kralchevsky, *J. Colloid and Interface Sci.* **405**, 269 (2013).
  - [29] N. Aubry, P. Singh, M. Janjua, and S. Nudurupati, *Proc. Nat. Acad. Sci.* **105**, 3711 (2008).
  - [30] K. D. Danov and P. A. Kralchevsky, *J. Colloid and Interface Sci.* **405**, 278 (2013).
  - [31] K. Zahn, J. M. Méndez-Alcaraz, and G. Maret, *Phys. Rev. Lett.* **79**, 175 (1997).